Chemical Engineering Journal 446 (2022) 137253

Contents lists available at ScienceDirect

Chemical Engineering Journal

journal homepage: www.elsevier.com/locate/cej

Green supported liquid membranes: The permeability activity-based linear operation (PABLO) method

Pablo López-Porfiri [a,*], María González-Miquel [a,b], Patricia Gorgojo [a,c,d,*]

[a] Department of Chemical Engineering, Faculty of Science and Engineering, The University of Manchester, Manchester M13 9PL, UK
[b] Departamento de Ingeniería Química Industrial y del Medioambiente, ETS Ingenieros Industriales, Universidad Politécnica de Madrid, C/ José Gutiérrez Abascal 2, 28006, Madrid, Spain
[c] Nanoscience and Materials Institute of Aragón (INMA) CSIC-Universidad de Zaragoza, C/ Mariano Esquillor s/n, 50018 Zaragoza, Spain
[d] Chemical and Environmental Engineering Department, Universidad de Zaragoza, C/ Pedro Cerbuna 12, 50009 Zaragoza, Spain

ARTICLE INFO

Keywords:
Supported liquid membrane (SLMs)
Green solvent
Organic acid
Biorefinery
Process design
COSMO-RS

ABSTRACT

Supported liquid membranes (SLMs) containing novel green solvents are proposed as a sustainable alternative separation process in the recovery of biomolecules. In this work, succinic acid has been successfully extracted from model fermentation broths through a stripping phase-facilitated transport mechanism with four different green supported liquid membranes: two eutectic solvents (DL-menthol:OctA and N_{4444}Cl:OctA), the bio-based solvent eucalyptol and the ionic liquid [C_4pyrr][Tf_2N]. A permeability activity-based model that takes into account for the first time solute-phase affinities has been developed using the quantum chemical COSMO-RS method; the model corrects the mass transfer driving force and allows extraction predictions beyond the concentration equilibrium. The best recovery has been achieved experimentally for the eucalyptol-based SLM (concentration factor of 1.4) using an alkaline aqueous solution (0.5 M NaOH) as the stripping phase. A countercurrent cascade extraction process design is proposed, and a graphical method to determine the stage number, interstage concentrations as well as mass transfer area requirements is presented. This new tool, the Permeability Activity-Based Linear Operation (PABLO) method, will substantially enhance the process design of SLMs technology for the biorefinery industry.

1. Introduction

Nowadays, concerns over climate change have led to stricter environmental regulations in the manufacturing processes, emphasizing the need to develop green chemistry alternatives [1]. However, green processes are often hard to implement at industrial scale due to the lack of technical maturity as well as economic, organizational, and even cultural barriers [2]. Examples of successful green processing facilities are the biorefineries, that transforms biomass into value-added products, yet most downstream separations in the industry still rely on the use of conventional processes to reach a competitive product quality and production cost.

For instance, the production of succinic acid and other bio-based organic acids, highlighted as strategic platform chemicals by the United States Department of Energy [3], through green routes has shown economically competitive in comparison to the conventional analogues [4]. However, the need to improve the downstream processes is also stressed. In fact, the purification of the bio-succinic acid produced by fermentation of lignocellulose-derived sugars is carried out by highly energy consuming precipitation processes or using harmful volatile organic compounds (VOCs), such as organophosphorus compounds or aliphatic amines, in liquid–liquid extractions (LLX) [5].

Novel technologies and materials are being proposed as sustainable alternatives or process intensification. Several ionic liquids (IL), i.e., liquid salts at room temperature, eutectic solvents (ES), i.e., hydrogen bond donor (HBD) and acceptors (HBA) eutectic mixtures, and bio-based solvents (BS), i.e., solvents produced from renewable sources, have shown to be suitable alternatives in LLX of bio-based organic acids [6]. Other energy efficient separation processes in the biorefinery industry can benefit from including the use of membranes, which are up to an order of magnitude more efficient than their phase change-based counterparts [7].

Liquid Membrane (LM) technology has been presented as an innovative approach for the selective extraction of diluted species from liquid or gaseous matrices, including the recovery of biomolecules,

* Corresponding authors at: Department of Chemical Engineering, Faculty of Science and Engineering, The University of Manchester, Manchester M13 9PL, UK.
E-mail addresses: pablo.lopezporfiri@postgrad.manchester.ac.uk (P. López-Porfiri), pgorgojo@unizar.es (P. Gorgojo).

https://doi.org/10.1016/j.cej.2022.137253
Received 21 April 2022; Received in revised form 25 May 2022; Accepted 26 May 2022
Available online 28 May 2022

Nomenclature

Symbols

$\Delta a_{m\ LM}$	Activity gradient logarithmic mean (mol·m^{-3})
a	Molar activity (mol·mol^{-1})
A	Membrane effective area (m^2)
a^{op}	Operating line intercept
a_m	Activity (mol·m^{-3})
b^{op}	Operating line slope
C	Concentration (mol·m^{-3})
c	Molar concentration (mol·mol^{-1})
D	Diffusion coefficient (m^2·s^{-1})
E	Extract phase
E_a	Arrhenius equation activation energy (J·mol^{-1})
E_f	Extraction factor (%)
Ex	Extraction yield (%)
F	Feed phase
h	Heat transfer coefficient (kW·m^{-2}·K^{-1})
J	Mass flux (mol·m^{-2}·s^{-1})
K	Thermal conductivity (kW·m^{-1}·K^{-1})
K'_D	Distribution coefficient (−)
L	Membrane length (m)
M	Mass flow (kg·s^{-1})
n	Solute mass (mol)
P	Permeability (m·s^{-1})
q	Solute flow (mol·s^{-1})
Q	Heat transfer Q (kJ·kg^{-1})
R	Raffinate phase
r^2	Pearson correlation coefficient
S	Stripping phase
T	Temperature (K)
t	Time (s)
u	Molecular mobility
$U_{comb,95\%}$	Combined expanded uncertainty
V	Volume (m^3)
x	x-axis length (m)
X	Solute-free solvent mass concentration

Constants

R	Gas constant = 8.314 (J·mol^{-1}·K^{-1})

Greek letters

α	Phase α
γ	Activity coefficient (−)
δ	Membrane thickness (m)
ε	SLM impregnation ratio (%)
μ	Chemical potential (kJ·mol^{-1})
ρ	Density (mol·m^{-3})
ψ	Linearized permeability model dependent variable value (−)

Superscripts

eq	Equilibrated
max	Maximum
st	Steady time

Subscripts

I	Component *i*
j	Data-point number
k	Dataset number
s	Phase solvent
T	Total

amino acids, metal ions, and rare earths, as well as the treatment of wastewater, nuclear waste, and removal of heavy metals [8]. By including an immiscible solvent within the porosity of an inert thin substrate in the so-called supported liquid membranes (SLM), allows to reduce the extraction media requirement and thereby the mass transfer resistance [9]. Furthermore, they can be coupled with green solvents to guarantee the sustainable requirements by the biorefinery industry. By comprising the extraction and back-extraction in a single stage, SLMs offer higher efficiency and simplest operation than LLX [10], even reaching a large mass transfer area per equipment volume [11].

Notwithstanding, despite the large number of published studies on LMs and the well acknowledged advantages, the technology is far from reaching industrial scale. In a separation roadmap report, formulated in the year 2000 by the American Institute of Chemical Engineers, the need for the development of alternative technologies was brought forward, highlighting the bio-separations as one of the highest priority key research needs [12]. Moreover, they specifically mentioned the importance of focusing on the development of membranes and extractants, as well as generating better predictive models to boost the separation technologies. The same conclusion was given in 2019 by the ACS Green Chemistry Institute® in a Sustainable Separation Processes Roadmap report [13].

The state of these separation methods can be overviewed from a technology maturity perspective. In order to visualize and compare different separation technologies, Fig. 1 shows their position with respect to each other, in terms of use maturity (antiquity) and from less sophisticated ones up to more sophisticated and well-stablished processes (technical sophistication, estimated from the wane in their respective patent activity). It is noted that LMs is a relatively young technology with a still high invention rate, which explains the poor industrial-scale development but leaves room for improvement and

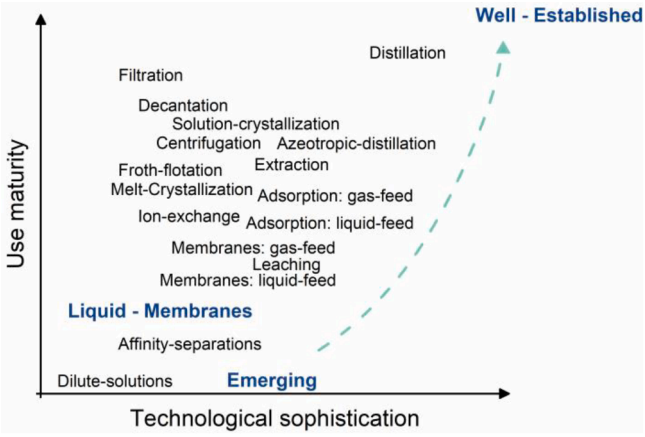

Fig. 1. Maturity of the separation process technology. Technological sophistication as the patent activity wane (*x*-axis); Use maturity as the antiquity in the last century (*y*-axis). Reconstructed from *Vision 2020: 2000 Separation Roadmap*, Center for Waste Reduction Technologies of the AIChE, 2000 [12].

developing the solutions the biorefinery industry is aiming for.

Under the proper conditions, several studies have shown that it is possible to push the LM extraction yields beyond the equilibria, i.e., to reach in the stripping phase a greater concentration than in the feed phase. For instance, it was reported that LMs based on Aliquat 336® could reach concentration factors of 2.2 and 6.9 in the gibberellic acid recovery [14] and uranium removal [15], respectively. In another work, lithium extraction from complex aqueous mixtures with IL-based SLM at

an initial Li concentration of 619 mg·l^{-1} showed to reach final concentrations of ca. 180 and 400 mg·l^{-1}, in the feed and striping phase, respectively [16]. This is possible due to reactive-facilitated mechanisms or specific solute–phase solvent affinities, and generally explained by the solute thermodynamic activity. However, discussions lack further insight or quantification, possibly due to time and cost constrains for the determination of thermodynamic properties.

In this work, we propose the use of computational quantum chemical methods to have a preliminary insight into such interaction effects. More precisely, the COnductor-like Screening MOdel for Real Solvents (COSMO-RS), which provides good predictions of compounds chemical potentials from the screening charge density on the molecular surface [17]. This unveils a potential improvement in the LM mass transfer description based on intermolecular interactions within the system and, in consequence, promoting further process modelling and design. The model will be validated with experimental data from the extraction of succinic acid using four SLMs based on four different green solvents: DL-menthol:OctA (eutectic solvent), N_{4444}Cl:OctA (eutectic solvent), eucalyptol (bio-based solvent) and [C_4pyrr][Tf_2N] (ionic liquid).

In order to reach technological maturity, it is necessary to develop tools that allow preliminary SLMs-based extraction process design (as those used for conventional separation technologies). In this work, a graphical method is proposed for the preliminary countercurrent configurations sizing.

2. Permeability activity-based model

In order to impulse LMs from an emerging to a well-established technology, descriptive models and process design methodologies must be improved. In LMs, the well-accepted mass transfer driving force is the concentration difference [18,19]. Assuming no solute accumulation within the membrane, the solute i flux, J_i (mol$_i$·m^{-2}·s^{-1}), is driven by the difference in concentration, C_i^{α} (mol·m^{-3}), between both phases (α: feed (F) or stripping (S)), and also depends on the permeability, P (m·s^{-1}). Thus, J_i can be calculated with equation (1) [20].

$$J_i = P\cdot\left(C_i^F - C_i^S\right) \tag{1}$$

The above approach is limited to describing the mass transfer only until both phase concentrations are equalized. Therefore, a new model needs to be developed to account for higher extraction efficiencies that can be found in the literature and go beyond the expected equilibrium.

In this work, the solute mass flux is expressed as a modified version of the Nernst–Planck equation, according to equation (2). The electrostatic potential is dismissed, resulting in a driving force along with a one-dimensional frame through the x-axis given by the chemical potential, μ_i (J·mol^{-1}), gradient. The other two terms in the equation are the solute activity, a_m (mol$_i$·m^{-3}), that accounts for molecular interactions within the mixture, and the molecular mobility, u.

$$J_i = a_m\cdot u\left(-\frac{d\mu_i}{dx}\right) \tag{2}$$

Based on the chemical potential relationship with the molar activity, a_i (mol$_i$·mol^{-1}), shown in equation (3) [21], and substituting $a_m = C_i\cdot\gamma_i$ as $a_m = c_i\cdot\rho\cdot\gamma_i$, where C_i (mol$_i$·m^{-3}), c_i (mol$_i$·mol^{-1}), γ_i (-), and ρ (mol·m^{-3}) are the solute molar concentration, the molar fraction, the activity coefficient, and the solution molar density, respectively, equation (2) can be rewritten as equation (4). The factor uRT, molecular mobility times the gas constant, R (J·mol^{-1}·K^{-1}), and temperature, T (K), is redefined as the solute diffusion coefficient, D (m^2·s^{-1}), resembling a Fick's law of diffusion based on the solute activity differential.

$$d\mu_i = RTdln(a_i) = RTdln(c_i\cdot\gamma_i) \tag{3}$$

$$J_i = -a_m\cdot uRT\frac{dln(a_i)}{dx} = -\frac{a_m}{a_i}\cdot D\frac{da_i}{dx} = -D\frac{d(C_i\cdot\gamma_i)}{dx} \tag{4}$$

Finally, the solute flux through the LM is obtained from the difference in each phase of the solute concentration times the activity coefficient and the permeability, P (m·s^{-1}), defined as the quotient of the diffusion coefficient over membrane thickness, δ (m), as shows equation (5). It is important to note that this approach considers no solute accumulation in the membrane and condenses all mass transfer resistances as a single empirical parameter P.

$$J_i = P\cdot\left(C_i^F\cdot\gamma_i^F - C_i^S\cdot\gamma_i^S\right) \tag{5}$$

Throughout the proposed permeability activity-based model, equation (5), the description of the LM process extraction is substantially improved. Wherever the separation process is, the final concentrations that it might reach are governed by the thermodynamic equilibria. In other words, when the activity of the compounds in each phase are equalized, also are the mass flow in both directions, meaning a zero-net mass transfer rate. For instance, if both feed and stripping phases are composed of the same solvent, e.g., water, no difference in the solute activity is observed, and the system will follow an ideal approach as per equation (1). In this case, both solute concentration trajectories, in feed and stripping phases, are constrained to meet over the same path, as shown the Fig. 2.I. In such figure, the a-point and b-point represent the initial feed and stripping concentrations, respectively, while the c-point is the final concentration of both phases obtained from the solute mass balance. Since the driven force of the ideal approach is the concentration gradient, the mass transfer is equilibrated at the c-point, as Fig. 2.II depicts.

On the other hand, under the activity-based approach, the solute trajectories are dependent on the specific solute-phase affinity. It is possible to attain equilibrium with different final concentrations, if different feed and stripping phases are adopted, such as water and a solution of 0.1 M NaOH, respectively. This case is illustrated in Fig. 2.III, where starting concentrations (a-point and b-point) are the same as in the above example, but the final feed concentration, d-point, is lower than the final stripping concentration, e-point, where the activities are balanced. In consequence, the observed concentration profiles behavior will match the one represented in Fig. 2.IV, agreeing with the results found in the literature.

3. Bio-organic acid recovery with green-SLMs

3.1. Materials

Succinic acid (≥99.0%$_{w/w}$), octatonic acid (≥98%$_{w/w}$), tetrabutylammonium chloride (>98%$_{w/w}$), 1,8-cineole (99%$_{w/w}$), and [C_4pyrr][Tf_2N] (≥98.5%$_{w/w}$) were purchased from Sigma-Aldrich. DL-menthol (≥97.0%$_{w/w}$) and NaOH (98%$_{w/w}$) were purchased from Alfa Aesar. Chemicals were used without further purification. Milli-Q type 1 water was produced in the laboratory. Millipore Durapore PVDF support was acquired from Merck. Nominal support characteristics are thickness: 125 μm, pore size: 0.22 μm, and porosity: 75%.

3.2. Preparation of green-SLMs

For the preparation of the SLMs, four green solvents (shown in Table 1) were selected based on their separation performance for the recovery of succinic acid through conventional LLX reported in our previous work [6]: two eutectic solvents (ESs) (DL-menthol:OctA and N_{4444}Cl:OctA), the bio-based solvent eucalyptol, and the ionic liquid (IL) [C_4pyrr][Tf_2N]. They were introduced into hydrophobic polyvinylidene fluoride (PVDF) porous supports by impregnation (Fig. 3.I and preparation details in the SI). Table 1 also contains the SLM impregnation ratio, $\varepsilon = V_{sovent}/V_{SML}$ (%), and stability in water for each of the prepared membranes (more details on these tests can be found in the SI).

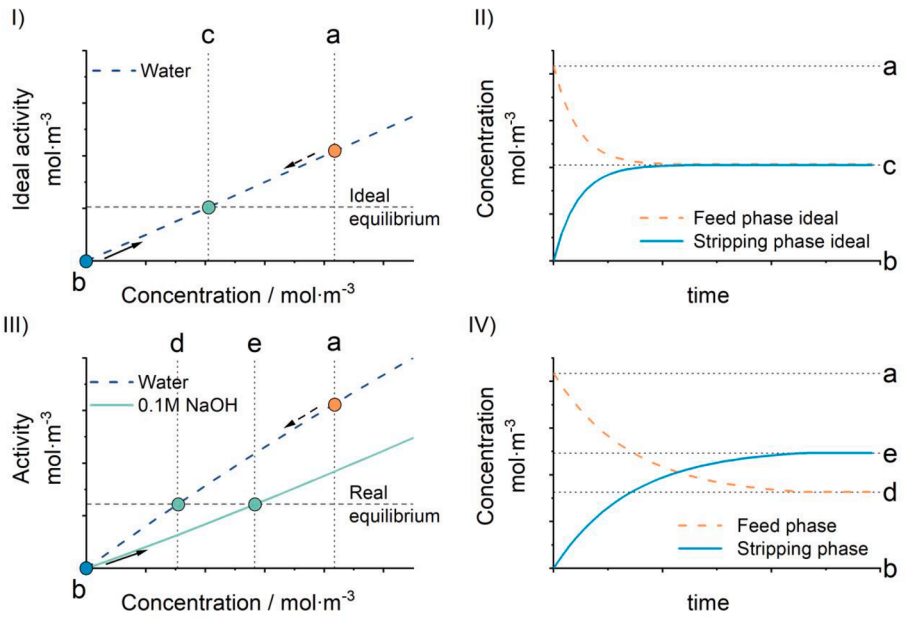

Fig. 2. Schematic comparison of the liquid membrane behavior predicted from a concentration-based approach (eq. (1)) and an activity-based approach (eq. (5)). I) Ideal trajectories for the solute concentration with the same affinity with the feed and stripping phases; II) Concentration profile obtained from the concentration-based approach; III) Activity trajectories for the solute concentration with different affinity with the feed and stripping phases; IV) Concentration profile obtained from the activity-based approach. *a*-point: initial feed concentration; *b*-point: initial stripping concentration; *c*-point: final ideal feed and ideal stripping concentration; *d*-point: final activity-based feed concentration; *e*-point: final activity-based stripping concentration.

Table 1
Green-SLM and their properties studied in this work.

Green solvent	Type	Abbreviation	ε	Stability [b]
			%	% at 96 h
DL-menthol: Octanoic acid {1:1}[a]	ES	DL-menthol: OctA	66.0 ± 2.7	94.29 ± 1.12
Tetrabutylammonium chloride: Octanoic acid {1:2}[a]	ES	N_{4444}Cl:OctA	66.1 ± 2.0	90.34 ± 1.28
1,8-Cineole	BS	Eucalyptol	66.5 ± 0.6	98.18 ± 3.15
1-butyl-1-methylpyrrolidinium bis(trifluoromethylsulfonyl) imide	IL	[C_4pyrr][Tf_2N]	49.3 ± 1.8	63.09 ± 2.80

[a] ES {HBA:HBD} molar ratio.
[b] Full stability data available in SI.

3.3. Methodology for the extractions with SLMs

Succinic acid was used as representative bio-based organic acid for the green-SLM extraction assays. Experimental extractions were carried out at room temperature in the diffusion cell depicted in Fig. 3.II; volume of 325 ml for the feed and stripping phase chambers and an effective mass transfer area of 30.19 ± 0.01 cm^2. A model succinic acid aqueous solution of 40–50 $g{\cdot}l^{-1}$, within the typical average concertation in the fermentation broths [22], was used as the feed phase. Pure water, 0.1 M NaOH, and 0.5 M NaOH were used for the stripping phase. Both feed and stripping phases were continually stirred to reduce polarization effects. The organic acid concentration of the stripping phase was measured in time intervals up to 100 h to ensure equilibrium was reached. The succinic acid concentration was analyzed by HPLC.

3.4. Modelling procedure

To give a continuous description of the succinic acid concentration profile in time, the experimental data were modelled with the perme-

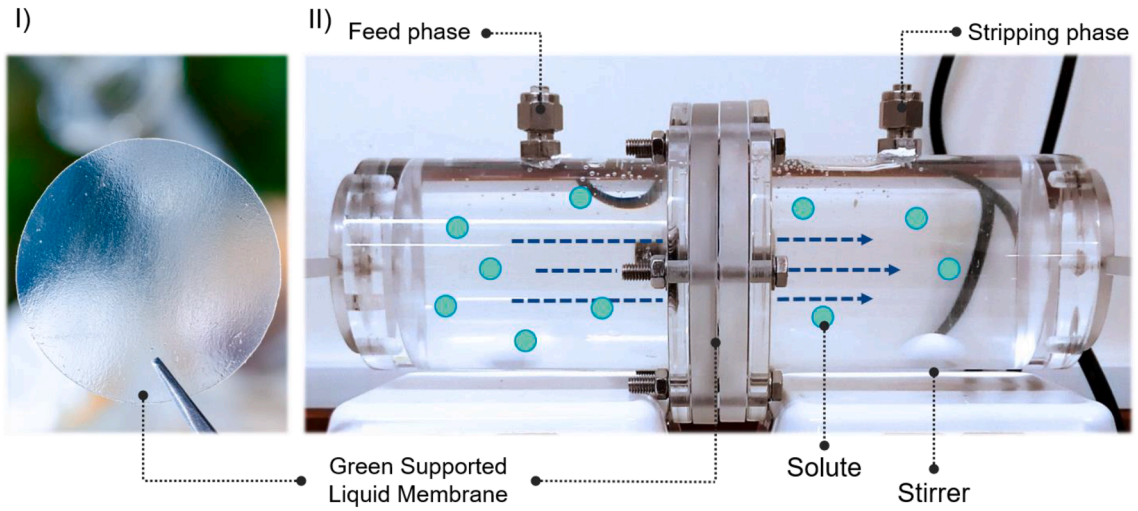

Fig. 3. Experimental setup used in this work for the succinic acid recovery with green-SLMs. I) SLM prepared by immersing a PVDF porous support in a green solvent; II) Diffusion cell and SLM module. (For interpretation of the references to colour in this figure legend, the reader is referred to the web version of this article.)

ability activity-based model proposed in this work. Since the approach is based on the solute-phase affinity, the succinic acid activity coefficients in water and NaOH solutions were preliminary computed with COSMO-RS method at 20 °C. The method has been successfully applied in the separation process design of complex systems [23] and in predicting the non-ideal carboxylic acids' aqueous solubilities [24]. By computing the compounds chemical potential within a mixture, COSMO-RS method can estimate the γ-values through equation (6), where μ_i^a and μ_i are the solute i chemical potential in the α-phase and as a pure compound, respectively [25]. Computational calculations were performed using the COSMOtherm software, version C30, release 18.0.2, at the parametrization of BP_TZVP_18.

$$RTln\left(\gamma_i^a\right) = \mu_i^a - \mu_i \tag{6}$$

The SLM configuration gives a negligible membrane phase volume in comparison with the feed and stripping phases. Therefore, the solute mass balance in the system described in Fig. 3.II can be expressed by equation (7). V^{α}, n^{α}, A, and t are the α-phase volume (m^3), solute mass (mol), membrane effective area (m^2), and extraction time (s), respectively.

$$J_i \cdot A = V^S \cdot \frac{dC_i^S}{dt} = -V^F \cdot \frac{dC_i^F}{dt} = \frac{dn_i^S}{dt} = -\frac{dn_i^F}{dt} \tag{7}$$

Assuming constant solute permeability throughout the concentration range (i.e., solute accumulation in the membrane is neglected), the permeability can be estimated from the mass balance formulated as equation (7), with experimental extraction data. With the boundary conditions of $0 < C^S(t) < C_i^{S,eq}$ and $t^{st} < t < t^{eq}$, the mass balance (equation (7)) and the permeability activity-based model (equation (5)) can be rearranged in the form: $y = b \cdot x + a$, as shown in equation (8). The linearized form establishes an independent variable $x = t$ and arises a dependent variable $y = \psi$. The initial condition is given at $C_i^S(t^{st}) = 0$ and $t = t^{st}$, the mass transfer steady-time (st), i.e., the time that the solute needs to fully permeate the SLM and start to desorb into the stripping phase. The final condition is reached when the system is equilibrated (eq), at $C_i^{S,eq}$ and t^{eq}, and the mass transport rate is ceased. The effective succinic acid permeability throughout the green-SLMs is determined from the function slope.

$$\frac{P \cdot A}{V^S} \cdot (t - t^{st}) = \frac{1}{V^S} \int_0^{C^S} \frac{dn^S}{\left(\frac{n^{F_{t=0}} - n^S}{V^F} \cdot \gamma^F - \frac{n^S}{V^S} \cdot \gamma^S\right)} = \psi \tag{8}$$

12 systems (1 solute × 4 green-SLM × 3 stripping phase) have been measured. To fit equation (8) to each experimental k dataset of j data-point number, both feed and stripping solute affinities must be corrected from COSMO-RS predictions. In total, there are three parameters to be fitted: γ_i^{Water}, $\gamma_i^{0.1MNaOH}$, and $\gamma_i^{0.5MNaOH}$. Since the parameter values must meet the equation (8) linearization, the objective function was established as the inverse sum of the squared Pearson correlation coefficient (r^2), according to equation (9). A MatLab® algorithm has been developed to obtain the solute activity coefficients (equations S3-S12 in the SI).

$$OF: \min\left[\sum_k \left\{\left(\frac{\sum_j \left\{\left(t_{j,k} - \bar{t}_k\right) \cdot \left(\psi_{j,k} - \bar{\psi}_k\right)\right\}}{\sqrt{\sum_j \left\{\left(t_{j,k} - \bar{t}_k\right)^2\right\} \cdot \sum_j \left\{\left(\psi_{j,k} - \bar{\psi}_k\right)^2\right\}}}\right)^2\right\}\right]^{-1} \tag{9}$$

Finally, the goodness of the model fit was determined by the root mean squared deviations from all experimental datasets, according to equation (10), where N is the total experimental data points.

$$RSMD = \sqrt{\frac{1}{N}\sum_k \sum_j \left(C_{j,k}^{exp} - C_{j,k}^{cal}\right)^2} \tag{10}$$

3.5. Results and discussion

Extraction of succinic acid from aqueous model solutions with green-SLM composed of DL-menthol:OctA, $N_{4444}Cl$:OctA, eucalyptol, or [C_4pyrr][Tf_2N] in PVDF supports were performed at room temperature. The measured concentrations over time have an average combined expanded uncertainty of $U_{comb,95\%}(C_i) = 1.67\ g \cdot l^{-1}$, estimated following the directions of Chirico et al. [26] and Miller and Miller [27] with a confidence level of 95%.

According to the preliminary COSMO-RS computational results, the succinic acid activity coefficient in NaOH solutions remains constant in neutral and low pH solutions, and significantly decreases for pH values over 12 (activity coefficient vs pH for succinic acid and other organic acids in Figure S4). The succinic acid concentration profile over time for the eucalyptol green-SLM with three different stripping phases (Fig. 4) reveals the expected behavior, i.e., greater concentrations as the pH of the receiving phase increases. Indeed, the average concentration factors resulted in 1.0, 1.1, and 1.4 for the membranes whose stripping solutions were water (pH 6–7), 0.1 M NaOH (pH 13.0–13.2), and 0.5 M NaOH (pH 13.5–13.7), respectively. The same behavior is observed for all green-SLM systems studied in this work (shown in Figure S5). This suggests that solute-phase affinities have a greater influence on the maximum process extraction capacity, while the solute-membrane affinity determines the mass transfer rate and therefore, the time needed to reach equilibrium.

Alkaline stripping solutions are commonly used to aid in the extraction of acid compounds from the membrane phase, due to the solute dissociation at a high pH that overcomes concentration gradients [28,29]. Moreover, the use of stripping phases of different nature allows tailoring the extraction selectivity in multistage separation processes, as demonstrated elsewhere for the separation of platinum and palladium from an aqueous mixture of the two components plus rhodium in a two-step process [30]. In such work, a stripping solution of 0.1 M $NaClO_4$ in 1 M HCl was first used to extract 96% of Pt(IV), and then a stripping solution of 10 mM thiourea and 0.1 M KSCN in 1 M HCl to extract 6% of Pd(II), with no Rd(III) extracted from the feed in neither of the two steps.

Graphs in Fig. 4 also show the ideal (equation (1)) and activity-based (equation (5)) models fitted to the experimental data. For the permeability activity-based model, the succinic acid activity coefficients were fitted following the procedure described in section 3.4. Fitted results, Fig. 5.I, indicates that the COSMO-RS method overestimates the differences in affinity but provides a correct trend prediction. When solute-phase affinities are alike, i.e., feed and stripping solution are the same (i.e., water in both phases), the ideal and the activity-based approaches, converge to equivalent trajectories. However, as the affinity gradient is increased, the concentration-based model keeps predicting the same ideal behavior, disagreeing with the experiment data. The RMSD (equation (10)) of both models are compared with the root mean squared deviations of the experimental uncertainty, as shown in Fig. 5.II. It is noted that the ideal model has a significant difference from the experimental measurements, while the fitted activity-based model shows better agreement to each data point.

Estimations of succinic acid permeabilities from both approaches are depicted in Fig. 6. The average combined expanded uncertainties are $U_{comb,95\%}(P^{ideal}) = 1.5x10^{-7}\ m \cdot s^{-1}$ and $U_{comb,95\%}(P^{acticty-based}) = 6.9x10^{-8}\ m \cdot s^{-1}$, respectively. Despite slightly better succinic extractions for the SLMs with 0.1 M NaOH as the stripping solution, the permeability in those systems tends to be smaller than with pure water. The addition of NaOH leads to an increase in the osmotic pressure of the receiving phase, and therefore, an extra mass transfer resistance for the solute desorption from the membrane. However, at higher NaOH concentrations of 0.5 M the succinic acid affinity gradient becomes the predominant effect over the osmotic pressure. Indeed, the most favorable extraction system for the succinic acid recovery is the eucalyptol-based SLM, despite its low permeability in comparison to other systems.

The above results highlight the importance of not treating complex

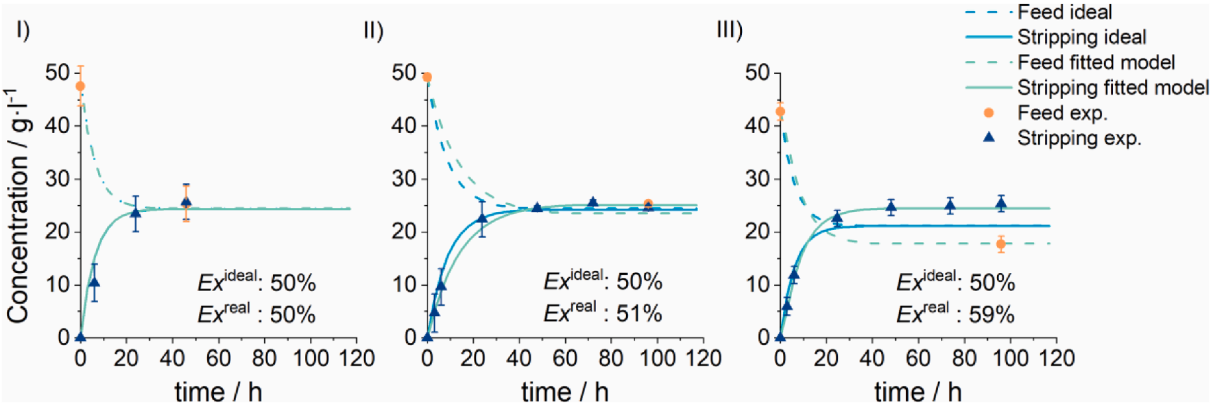

Fig. 4. Experimental, ideal (eq. (1)), and fitted permeability activity-based (eq. (5)) models concentration profile and extraction yields (*Ex*) for succinic acid extraction with a eucalyptol-based green-SLM and three different stripping solutions. I) pure water; II) 0.1 M NaOH; III) 0.5 M NaOH. The same behavior is observed for all green-SLM studied in this work. (For interpretation of the references to colour in this figure legend, the reader is referred to the web version of this article.)

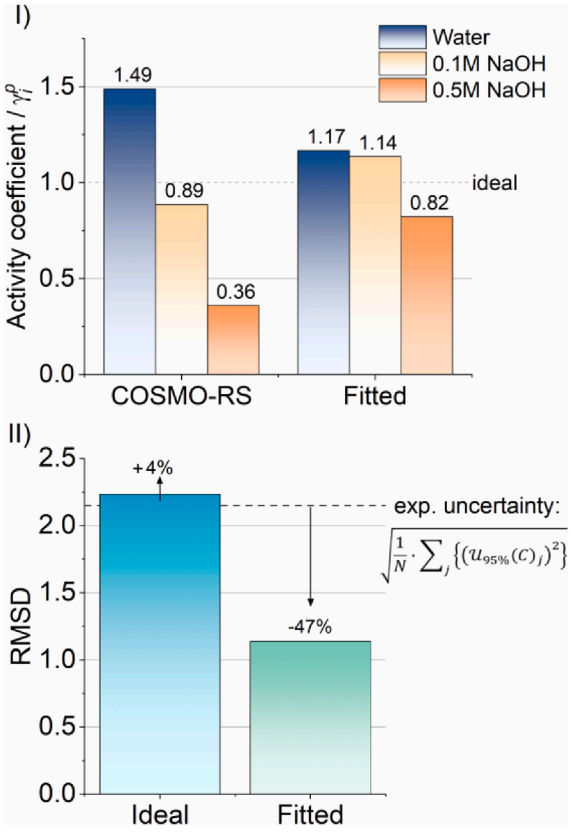

Fig. 5. I) Succinic acid activity coefficient in water and alkaline solutions predicted by the COSMO-RS method at 20 °C and fitted to the experimental extraction data with green-SLM and the permeability activity-based model proposed in this work; II) Root mean squared deviation comparison of the ideal and fitted permeability activity-based models. The goodness of the models is also evaluated through the root mean squared deviations of the experimental uncertainty with a confidence level of 95%. (For interpretation of the references to colour in this figure legend, the reader is referred to the web version of this article.)

interactions as an ideal system for the proper process description. Moreover, a misleading approach can have major consequences in the technology scale-up. Since the ideal model does not consider the activity correction in the concentration gradients, the permeability is overestimated. This might result in smaller equipment sizing that will not reach the expected extraction yields.

4. Cascade extraction process design

The extraction effectiveness in a separation process is governed by the thermodynamic equilibrium of the system. Given enough time and mass transfer area, the maximum possible solute extraction in a two-phase system is determined by the solute distribution coefficient, K'_D. The solute distribution coefficient establishes the solute concentration ratio in equilibrium between the feed (*F*) and the stripping (*S*) phase, each defined as the saturated solute mass over the solute-free solvent mass, $X_i^{S,eq}$. Rearranging it by the equilibria criteria, $a_m^{F,eq} = a_m^{S,eq}$, the distribution coefficient can be obtained from the ratio of the phase solvent density (ρ) times the solute activity coefficient (γ) in it, as shown in equation (11):

$$K'_D = \frac{X_i^{S,eq}}{X_i^{F,eq}} = \frac{\rho^{Solvent\ S}\cdot\gamma_i^S}{\rho^{Solvent\ F}\cdot\gamma_i^F} \tag{11}$$

Separation processes require K'_D above 1 to keep the mass transfer rate towards the extracting phase. Although operating with a large stripping to feed ratio allows to improve the extraction for systems with low K'_D, this implies a low final concentration in the extract. In practice, a single extraction stage often is not sufficient to reach process specifications, and multistage extraction processes are typically used [31]. There are several cascade separation process arrangements, e.g., cocurrent, countercurrent, and crosscurrent, being the countercurrent configuration the preferred one for liquid stream separations due to its high efficiency and lower number of stages required. In fact, multi-stage LM processes have shown high selectivity and extraction yields in a range of applications including the racemic amino acid enantioseparation [32], penicillin G recovery [33], and 2-chlorophenol removal [34].

Therefore, to improve the extraction capacity of SLMs, a countercurrent configuration of *N*-stages (Fig. 7) is proposed. The design is based on the equilibrium-stage model, considering the thermodynamic limitations discussed in previous sections. The feed (*F*) and stripping (*S*) streams, with initial solute concentrations C_F and C_S, respectively, are fed to each end of the process. It is assumed that the area and time within every stage are sufficient for the mass transfer to reach the equilibrium, i.e., solute activities in each stream are equalized. In an intermediate stage *n*, the raffinate stream coming out from the above stage (R_{n+1}) is treated with the extract of the stage below (E_{n-1}), helping to hold the mass transfer driving force.

4.1. Graphical activity-based process design

To determine the total number of stages (*N*) required in the proposed green-SLM countercurrent cascade process, a graphical method is derived from the permeability activity-based model seen in previous sections. The method, denoted as PABLO (Permeability Activity-Based Linear Operation) method, includes the following assumptions:

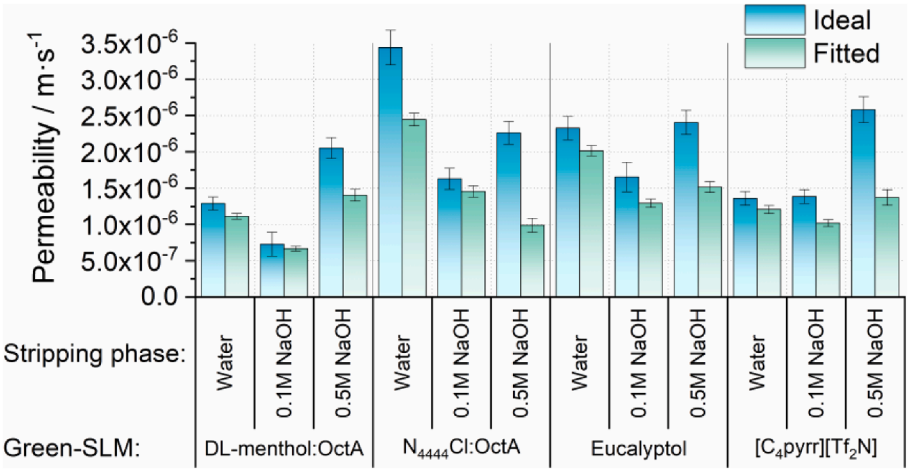

Fig. 6. Succinic acid permeability ($m \cdot s^{-1}$) for the green-SLM studied in this work with water and two alkaline aqueous solutions (0.1 and 0.5 M NaOH) as stripping phase obtained from the ideal and fitted permeability activity-based models. Error bars considered the value uncertainties with a confidence level of 95%. (For interpretation of the references to colour in this figure legend, the reader is referred to the web version of this article.)

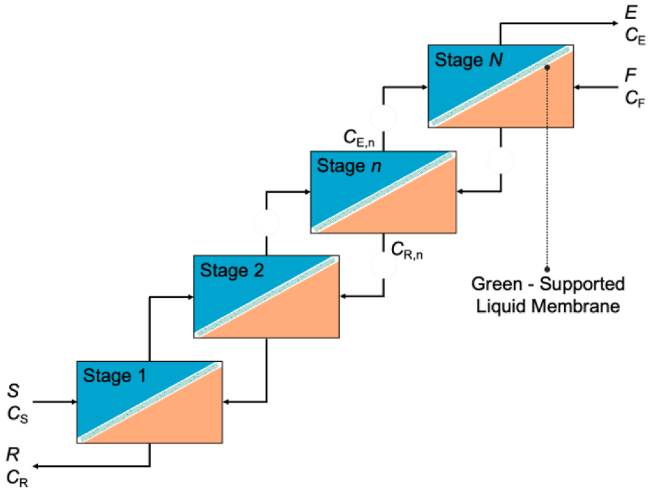

Fig. 7. Cascade green-SLM extraction process in a countercurrent flow diagram. *F*, feed stream; *S*, stripping stream; *R*, raffinate stream; *E*, extract stream; *N*, total stages number; *n*, stage number; C_F, initial solute concentration in the feed stream; C_S, initial solute concentration in the stripping stream; $C_{R,n}$, solute concentration in the raffinate for stage *n*; $C_{E,n}$, solute concentration in the extract for stage *n*; C_R, final solute concentration in the raffinate stream; C_E, final solute concentration in the extract stream. (For interpretation of the references to colour in this figure legend, the reader is referred to the web version of this article.)

- Constant activity coefficients and permeability within the concentration range.
- Equilibrium is reached in each stage.
- Negligible solute retained within the LM phase.
- Negligible water and pH-modifier transport.
- Negligible phase volume changes.
- Isothermic process.

The following operating parameters were selected for assessing the accuracy of the graphical method: concentration of succinic acid in the feed $C_F = 50\ g \cdot l^{-1}$, an alkaline 0.5 M NaOH stripping solution with no solute ($C_S = 0\ g \cdot l^{-1}$), and a feed to stripping phase ratio $S/F = 0.5$ (Table 2). The activity coefficient values were fitted from the permeability activity-based model and experimental green-SLM extraction measurements (see Fig. 5) presented in section 3.5. Nevertheless, feeding the model with purely empirical solute activity coefficients values might improve its capacity to predict the extraction behavior and thus the process design.

Table 2
Operating conditions and target final concentrations for the succinic acid recovery with green-SLM in a countercurrent cascade process.

	Phase:	Feed	Stripping
	Solvent:	Water	0.5 M NaOH
Solute Activity coefficient (γ)	–	1.17	0.82
Solvent density ($\rho^{Solvent}$)	$kmol_s \cdot m^{-3}$	55.4	55.9
Flow rate	$m^3 \cdot h^{-1}$	1.0	0.5
Initial concentration (*C*)	$g \cdot l^{-1}$	50	0
Solute free-based concentration (*X*)	$mol_i \cdot mol_s^{-1}$	0.008	0
Target final concentration (*C*)	$g \cdot l^{-1}$	16.5	67.0

The extraction factor, E_f (%), is defined as the distribution coefficient times the initial solute mass flow ratio, M^S/M^F (equation (12)). The theoretical maximum possible concentration in the extract stream (C_E^{max}) is calculated with equation (13). In a process design, the target final concentration in the extract stream must be set below the theoretical maximum in order to obtain a reasonable stage number and mass transfer area. The solute *i* recovery (X_i^R/X_i^F) in a countercurrent cascade with *N*-stages can be obtained from the process mass balance and the E_f value, according to equation (14), [31].

$$E_f = K_D^{'} \cdot \frac{M^S}{M^F} = K_D^{'} \cdot \frac{S \cdot \left(1 - X_i^S\right)}{F \cdot \left(1 - X_i^F\right)} \cdot \frac{\rho^{Solvent\ S}}{\rho^{Solvent\ F}} \tag{12}$$

$$C_E^{max} = \frac{F}{S} \cdot C_F \cdot E_f \tag{13}$$

$$\frac{X_i^R}{X_i^F} = \frac{1}{\sum_{n=0}^{N} \left(E_f\right)^n} \tag{14}$$

The distribution coefficient (equation (11)) and the extraction factor (equation (12)) for the system under the selected operating conditions results in $K'_D = 1.4$ and $E_f = 71.5\%$, respectively. According to equation (13), a maximum possible final concentration in the extract stream of $C_E^{max} = 71.5\ g \cdot l^{-1}$ could be obtained. The solute recovery vs total number of stages is shown in Fig. 8. It can be seen that extra stages do not lead to significant improvements when the recovery approaches the E_f value. Therefore, an optimum target value must be determined from the specific process objectives and constraints. When the target final solute concentration in the extract is set as $C_E = 67\ g \cdot l^{-1}$ five stages are needed, and the final concentration in the raffinate (calculated from the global mass balance) results in $C_R = 16.5\ g \cdot l^{-1}$.

Intermediate concentrations (C_{Rn} and C_{En}) are given by the operating

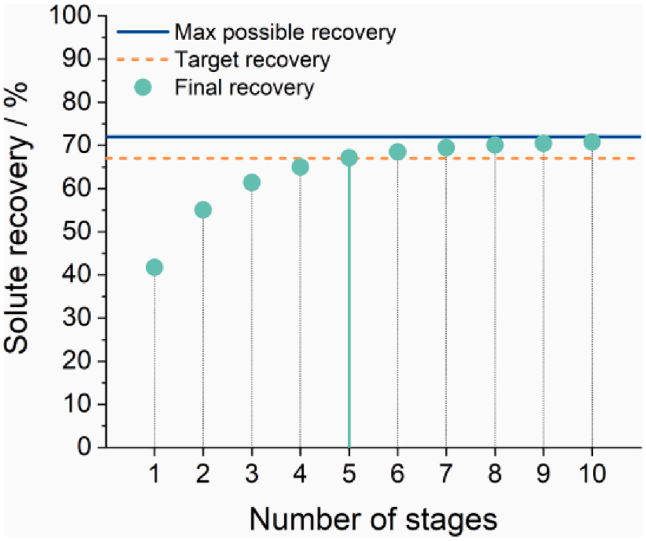

Fig. 8. Solute (succinic acid) recovery as a function of the number of stages in a countercurrent cascade at operating conditions listed in Table 2 (analytical resolution). The solute recovery converges to an upper limit given by the system thermodynamic equilibrium. To reach a target final concentration $C_E = 67$ g·l^{-1}, a five-stage extraction process is required.

solute activity trajectory a_m^{op}: the stripping phase solute trajectory corrected by the flowrate ratio as well as the initial and target concentrations. The operating line is defined as a linear function of the operating concentration (C_i^{op}), as expressed in equation (15). Operating line slope (b^{op}) and intercept (a^{op}) are given by equations (16) and (17), respectively.

$$a_m^{op} = C_i^{op} \cdot b^{op} + a^{op} \tag{15}$$

$$b^{op} = \gamma_i^S \cdot \frac{F}{S} \tag{16}$$

$$a^{op} = \gamma_i^S \cdot \left(C_E - \frac{F}{S} \cdot C_F \right) \tag{17}$$

Fig. 9 shows the graphical algorithm to obtain the required number of stages and interstage solute concentrations for the countercurrent cascade process with green-SLM coupled with the permeability activity-based model proposed in this work. The activity trajectories and operating line plot are built from the solute activity coefficients in the feed and stripping phases Fig. 9.I). C_F is the starting point, from which to descend vertically until the operating line is reached; the intersections of an horizontal line from that point with the feed and stripping phases trajectories give the raffinate and extract concentrations, respectively, for that stage (Fig. 9.II). The same procedure is repeated starting from the new C_{Rn} until reaching the final C_R concentration. The total number of stages is given by the number of steps taken to complete the algorithm (Fig. 9.III).

The proposed graphical activity-based procedure predicts 5 stages for the conditions defined in Table 2 (see Fig. 9.III), which agrees with the calculated from of the analytical method (equation (14)). The overall succinic acid recovery results in 67%. The graphical method is capable of determining the interstage activity profile. The driving force for the mass transfer, i.e., the activity gradient between the feed and the stripping phases, is maintained along the process as seen in Fig. 10.I. This enhances the extraction going in an uphill concentration flux, where the final extract concentration is greater than the initial feed stream, as it is shown in the interstage concentration profile in Fig. 10.II.

4.2. Required green-SLM area estimation

Equipment sizing is a key aspect in process design to perform both technical and economic evaluations. For SLM separation technology, this means to determine the effective mass transfer surface area to assess material, solvent, and apparatus costs.

In order to estimate the required mass transfer area to carry out the extraction with the green-SLM countercurrent cascade design described above, the following procedure is proposed. The transported solute flow, q (mol·s^{-1}), throughout a membrane section, A (m^2), is described by equation (18). If a rectangular green-SLM geometry is assumed, the area section is defined as $dA = y \cdot dz$, where the section width (y) is constant and the activity gradient, Δa_m (mol·m^{-3}), only vary in the z-axis. Thus, the total transported solute within a fixed length (L) is determined by equation (19). A general expression of the Δa_m dependence along the z-axis is given by equation (20), as the activity gradient logarithmic mean, $\Delta a_{m\,LM}$ (mol·m^{-3}), it is based on the initial ($z = 0$) and final ($z = L$) extraction stage conditions. The formal $\Delta a_{m\,LM}$ derivation is found in the SI.

$$\frac{\partial q}{\partial A} = P \cdot \left(a_m^F - a_m^S \right) = P \cdot \Delta a_m \tag{18}$$

$$q = P \int_{z=0}^{z=L} \Delta a_m \cdot y dz \tag{19}$$

$$\Delta a_{m\,LM} = \frac{\left(a_m^F - a_m^S \right)_{z=0} - \left(a_m^F - a_m^S \right)_{z=L}}{ln\left(\frac{\left(a_m^F - a_m^S \right)_{z=0}}{\left(a_m^F - a_m^S \right)_{z=L}} \right)} \tag{20}$$

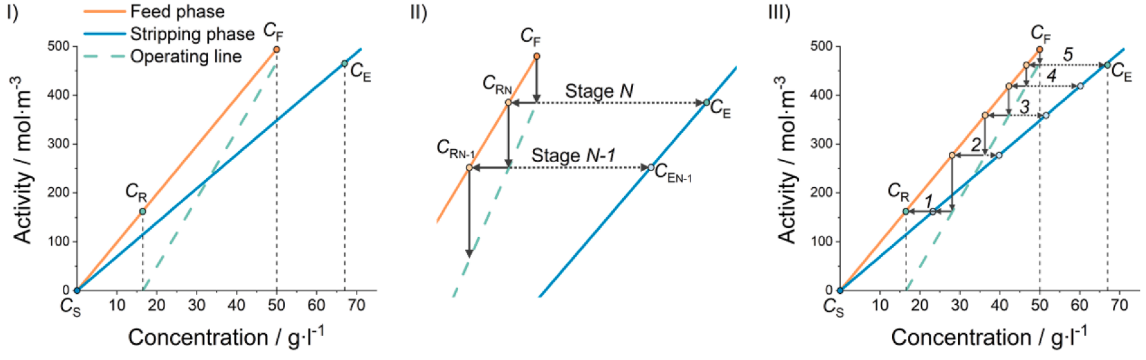

Fig. 9. Green-SLM countercurrent cascade extraction process graphical algorithm (PABLO) to determinate the number of stages required to reach the target final concentration by the permeability activity-based linear operation. I) Activities trajectories of the solute in the feed and stripping phases as well as the operating line obtained from the respective solute activity coefficient in each phase and the process operating conditions through eq. (15) to eq. (17); II) Stage number determination procedure: vertically descending from the initial feed concentration, C_F, to the operation line, then spitted horizontally towards the feed, C_{Rn}, and stripping, C_E, lines. Repeat the procedure from, C_{RN}, until reaching the final concertation in the raffinate, C_R; II) Total number stages as the step number required to reach the final raffinate concentration, obtained under the operational condition listed in Table 2. (For interpretation of the references to colour in this figure legend, the reader is referred to the web version of this article.)

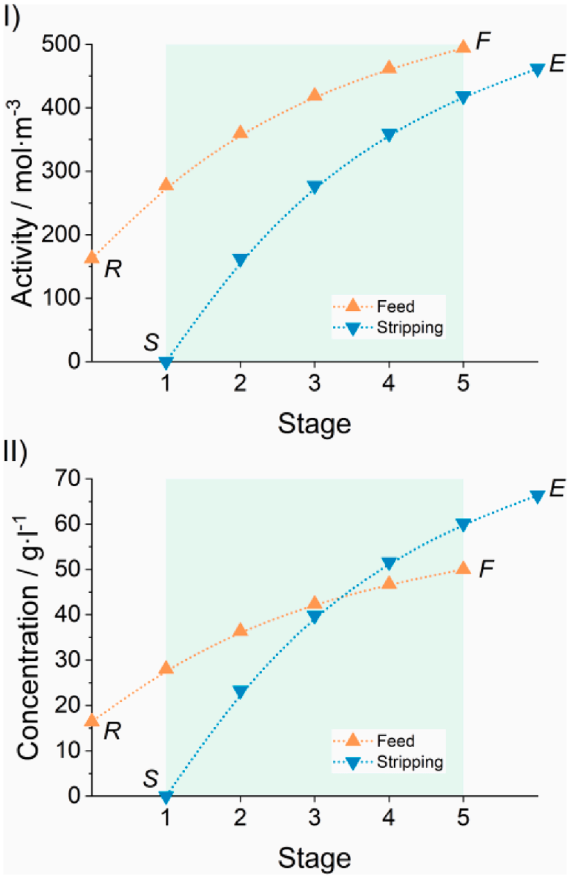

Fig. 10. I) Activity profile and II) concentration profile of the succinic acid throughout a countercurrent cascade five-stages green-SLM extraction obtained from the permeability activity-based model proposed in this work. A solution of 0.5 M NaOH is used as stripping phase. *F*: feed stream; *S*: stripping stream; *R*: raffinate stream; *E*: extract steam. Lines were included to guide the eye. (For interpretation of the references to colour in this figure legend, the reader is referred to the web version of this article.)

The required stage green-SLM area (A is determined from equation (21), where the activity values can be obtained from the activity profile (see Fig. 10.I) derived from the graphical permeability activity-based method described in section 4.1. The total area, A_T (m^2), of an *n*-stages countercurrent cascade extraction process is given by equation (22).

$$A = \frac{q}{P \cdot \Delta a_{m\,LM}} \tag{21}$$

$$A_T = \frac{1}{P}\sum_{n=1}^{N} \frac{q_n}{\Delta a_{m\,LM,n}} \tag{22}$$

The required area (total and for each of the countercurrent cascade stages) with the four different green-SLM studied in this work is shown in Fig. 11. The total area is inversely proportional to the solute permeability throughout the green-SLM (see Fig. 6). For the same operating conditions and number of extraction stages, values of equipment size show significant differences. Although experimental results exhibited others succinic acid extraction systems with larger permeability, e.g., using pure water as the stripping phase, their final concentration factor capacity was reduced, meaning smaller equipment but lesser final extract concentration. This evidences the importance to consider the systems thermodynamic capacity to extract the target solute and the SLM mass transport performance as a coupled effect in the process development.

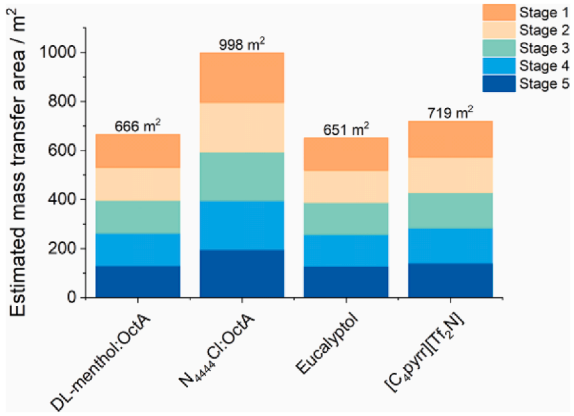

Fig. 11. Estimated total and by stage mass transfer area for the extraction of succinic acid in a five-stage countercurrent cascade extraction process using an alkaline aqueous solution (0.5 M NaOH) as the stripping phase and four different green-SLM. (For interpretation of the references to colour in this figure legend, the reader is referred to the web version of this article.)

4.3. Temperature-driven green SLM extraction

In previous sections it has been modelled and demonstrated experimentally that adding a pH modifier can favor the extraction of an organic acid through SLMs. However, in some cases, this strategy might not be possible due to incompatibilities with the process or interferences in further purification stages.

The solute activity coefficient is not only a property dependent on the system conformation but on the temperature as well. This presents an opportunity for further studies on the SLM technology process design based on temperature gradients as an alternative way to control the solute affinity within the system. Temperature-driven processes are well known in membrane separation technologies. One examples is membrane distillation (MD), another emerging separation method that benefits from stream temperature differences to enhance the *trans*-membrane vapor flux in water recovery [35,36].

The affinity temperature dependency can be reliably described by empirical activity coefficient models, such as the Non-Random Two Liquid model (NRTL) [37]. Based on the system excess Gibbs energy calculations, the NRTL model allows the activity coefficients determination as a function of the temperature and mixture composition. Fig. 12.I shows the succinic acid activity in pure water represented by the NRTL model computed by COSMO-RS method. At high acid concentration and temperature, greater activity is observed with a non-linear dependency. Thus, a counterflow extraction process of a hot feed stream and a cold stripping stream will effectively promote the solute mass transfer.

In this arrangement, the mass and heat transfer are coupled phenomena. On the one hand, both the mass transfer resistances, ab/desorption rates and solute diffusion, as well as the driving force, solute chemical potential, are temperature-dependent factors. Thus, permeability must be corrected along with the heat exchange. The permeability as a temperature function is expressed in an Arrhenius-form equation (equation (23)), based on an empirical parameter, E_a ($J \cdot mol^{-1}$), representing the activation energy [38]. On the other hand, given a membrane area and temperature gradient, ΔT (K), the heat transfer, Q ($kJ \cdot kg^{-1}$), throughout the membrane is determined from equation (24). The heat flow is dependent on the convective heat transfer coefficient, h ($kW \cdot m^{-2} \cdot K^{-1}$), of each stream, the membrane thickness, δ (m), and membrane thermal conductivity, k ($kW \cdot m^{-1} \cdot K^{-1}$). For membrane conductive heat transfer, an isostrain model can be used to estimate the two-phase composite material SLM thermal conductivity, according to equation (25), weighing the support and solvent thermal conductivity by the SLM impregnation ratio, ε (%) [39].

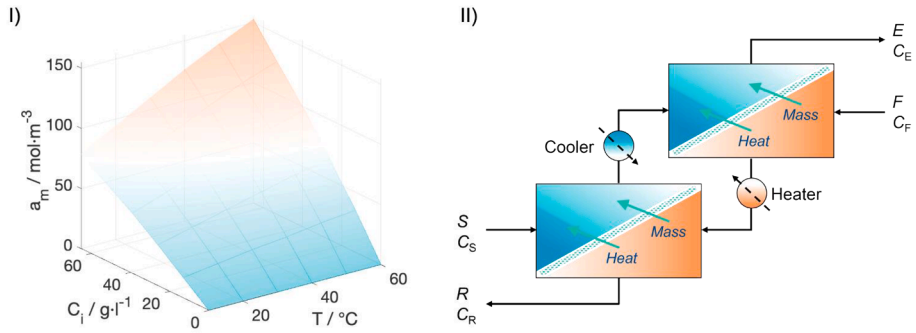

Fig. 12. I) Succinic acid activity dependence with concentration and temperature computed with COSMO-RS method and represented by the NRTL model; II) Schematic two-stage countercurrent cascade extraction process with intermediate cooler/heater auxiliary processes.

$$\frac{P_i(T_2)}{P_i(T_1)} = exp\left[-\frac{E_a}{R}\left(\frac{1}{T_2}-\frac{1}{T_1}\right)\right] \tag{23}$$

$$Q = \left[\frac{1}{h^F}+\frac{\delta}{k}+\frac{1}{h^S}\right]^{-1}\cdot A\cdot \Delta T \tag{24}$$

$$k = (1-\varepsilon)\cdot k_{support} + \varepsilon\cdot k_{solvent} \tag{25}$$

Fig. 12.II presents a schematic two-stage countercurrent cascade extraction process driven by the solute activity dependence on the temperature and concentration gradients. As both mass and heat are transferred from one stream to another, the temperature gradient is reduced after each extraction stage. Thus, to enhance the process efficiency, interstage heaters and coolers can be implemented to overcome the mass transfer rate drop. Despite the increased energy consumption, this effect can be efficiently managed through process energy integration methods between the cold and heat streams [40]. Note that this temperature-enhanced approach can be coupled with the facilitated transport mechanisms to reach an optimum extraction process design, opening up avenues to impulse the LM technology towards becoming one of the predominant separation methods among other well-established industrial processes.

5. Conclusions

The new permeability activity-based approach presented in this work fulfils a fundamental gap in the SLM process modelling. It allows overcoming the concentration-based models' limitations, as it predicts the final equilibrium state by accounting for solute activity effect. Experimental succinic acid recovery with four different green-SLM (DL-menthol:OctA and N_{4444}Cl:OctA eutectic solvents, the bio-based solvent eucalyptol and the ionic liquid [C_4pyrr][Tf_2N]) confirmed that extraction yields are determined by the solute-phase affinities, being the stripping phase pH the most relevant factor. Thus, a selective-oriented design can be performed establishing favorable compounds affinities. On the other hand, the SLM conformation has a major influence on the solute permeability, determining the mass transfer rate. Both effects are key for a proper SLM process design.

A graphical method, PABLO (Permeability Activity-Based Linear Operation), for calculating the theoretical number of stages required for the extraction of organic acids in a multistage countercurrent cascade design has been developed. The mass transfer area requirement, a critical parameter for assessing the techno-economic feasibility of the process, can be also calculated. Additionally, coupling mass and heat transfer phenomena into the green-SLM extraction process has been proposed.

The developed approach will allow researchers to address preliminary system selection for further studies and will help in the feasibility assessment of green solvents and SLMs for sustainable separation processes. Especially, it is foreseen as a tool for the biorefinery industry to implement competitive green routes into chemical manufacturing and work towards technological maturity.

Funding sources

This work was funded by the CONICYT PFCHA/DOCTORADO BECAS CHILE/2017 – 72180306. P. Gorgojo acknowledges the Spanish Ministry of Economy and Competitiveness and the European Social Fund through the Ramon y Cajal programme (RYC2019-027060-I/AEI/10.13039/501100011033). M. González-Miquel acknowledges Madrid Government (Comunidad de Madrid-Spain) for funding through the Multiannual Agreement with Universidad Politécnica de Madrid under the Excellence Programme for University Professors, in the context of the V PRICIT (Regional Programme of Research and Technological Innovation).

Declaration of Competing Interest

The authors declare that they have no known competing financial interests or personal relationships that could have appeared to influence the work reported in this paper.

Appendix A. Supplementary data

Supplementary data to this article can be found online at https://doi.org/10.1016/j.cej.2022.137253.

References

[1] V.R. Veleva, B.W. Cue, The role of drivers, barriers, and opportunities of green chemistry adoption in the major world markets, Curr. Opin. Green Sustain. Chem. 19 (2019) 30–36, https://doi.org/10.1016/j.cogsc.2019.05.001.
[2] F. Roschangar, R.A. Sheldon, C.H. Senanayake, Overcoming barriers to green chemistry in the pharmaceutical industry-the Green Aspiration Level™ concept, Green Chem. 17 (2015) 752–768, https://doi.org/10.1039/c4gc01563k.
[3] T.A. Werpy, J.E. Holladay, J.F. White, Top Value Added Chemicals From Biomass: I, in: Results of Screening for Potential Candidates from Sugars and Synthesis Gas, 2004, https://doi.org/10.2172/926125.
[4] J.M. Pinazo, M.E. Domine, V. Parvulescu, F. Petru, Sustainability metrics for succinic acid production: A comparison between biomass-based and petrochemical routes, Catal. Today. 239 (2015) 17–24, https://doi.org/10.1016/j.cattod.2014.05.035.
[5] L.M.J. Sprakel, B. Schuur, Solvent developments for liquid-liquid extraction of carboxylic acids in perspective, Sep. Purif. Technol. 211 (2019) 935–957, https://doi.org/10.1016/j.seppur.2018.10.023.
[6] P. López-Porfiri, P. Gorgojo, M. Gonzalez-Miquel, Green Solvent Selection Guide for Biobased Organic Acid Recovery, ACS Sustain. Chem. Eng. 8 (2020) 8958–8969, https://doi.org/10.1021/acssuschemeng.0c01456.
[7] D.S. Sholl, R.P. Lively, Seven chemical separations to change the world, Nature. 532 (2016) 435–437, https://doi.org/10.1038/532435a.
[8] P. López-Porfiri, M. González-Miquel, P. Gorgojo, Liquid Membrane Technology for Sustainable Separations, in: G. Szekely, D. Zhao (Eds.), Sustain. Sep. Eng., First Edit, Wiley, 2022: pp. 297–341. https://doi.org/10.1002/9781119740117.ch8.
[9] M.A. Malik, M.A. Hashim, F. Nabi, Ionic liquids in supported liquid membrane technology, Chem. Eng. J. 171 (2011) 242–254, https://doi.org/10.1016/j.cej.2011.03.041.
[10] V.S. Kislik, Liquid Membranes: Principles and Applications in Chemical Separations and Wastewater Treatment, 1st ed.,, Elsevier B.V, 2010.
[11] P.K. Parhi, Supported Liquid Membrane Principle and Its Practices: A Short Review, J. Chem. 2013 (2013) 1–11, https://doi.org/10.1155/2013/618236.

[12] S. Adler, E. Beaver, P. Bryan, S. Robinson, J. Watson, Vision 2020: 2000 Separations Roadmap, 2000. https://doi.org/10.2172/1218701.
[13] D.J.C. Constable, R. Giraud, A. Sehgal, D. Sullivan, Sustainable Separation Processes. A Road Map to Accelerate Industrial Application of Less Energy-Intensive Alternative Separations (AltSep), 2019.
[14] J. Berrios, D.L. Pyle, G. Aroca, Gibberellic acid extraction from aqueous solutions and fermentation broths by using emulsion liquid membranes, J. Memb. Sci. 348 (2010) 91–98, https://doi.org/10.1016/j.memsci.2009.10.040.
[15] N.S. Rathore, A.M. Sastre, A.K. Pabby, Membrane assisted liquid extraction of actinides and remediation of nuclear waste: A review, J. Membr. Sci. Res. 2 (2016) 2–13, https://doi.org/10.22079/jmsr.2016.15872.
[16] G. Zante, M. Boltoeva, A. Masmoudi, R. Barillon, D. Trébouet, Lithium extraction from complex aqueous solutions using supported ionic liquid membranes, J. Memb. Sci. 580 (2019) 62–76, https://doi.org/10.1016/j.memsci.2019.03.013.
[17] F. Eckert, A. Klamt, Fast solvent screening via quantum chemistry: COSMO-RS approach, AIChE J. 48 (2002) 369–385, https://doi.org/10.1002/aic.690480220.
[18] S. Chaturabul, W. Sriracha, T. Wannachod, P. Ramakul, U. Pancharoen, S. Kheawhom, Separation of mercury(II) from petroleum produced water via hollow fiber supported liquid membrane and mass transfer modeling, Chem. Eng. J. 265 (2015) 34–46, https://doi.org/10.1016/j.cej.2014.12.034.
[19] B. Swain, C. Mishra, J. Jeong, J. Lee, H.S. Hong, B.D. Pandey, Separation of Co(II) and Li(I) with Cyanex 272 using hollow fiber supported liquid membrane: A comparison with flat sheet supported liquid membrane and dispersive solvent extraction process, Chem. Eng. J. 271 (2015) 61–70, https://doi.org/10.1016/j.cej.2015.02.040.
[20] L.J. Lozano, C. Godínez, A.P. de los Ríos, F.J. Hernández-Fernández, S. Sánchez-Segado, F.J. Alguacil, Recent advances in supported ionic liquid membrane technology, J. Memb. Sci. 376 (1-2) (2011) 1–14.
[21] E.R. Cohen, I. Mills, H.L. Strauss, J.G. Frey, I. Mills, K. Homann, K. Kuchitsu, Quantities, units and symbols in physical chemistry, third edit, royal society of chemistry, Cambridge (2007), https://doi.org/10.1039/9781847557889.
[22] M. Jiang, J. Ma, M. Wu, R. Liu, L. Liang, F. Xin, W. Zhang, H. Jia, W. Dong, Progress of succinic acid production from renewable resources: Metabolic and fermentative strategies, Bioresour. Technol. 245 (2017) 1710–1717, https://doi.org/10.1016/j.biortech.2017.05.209.
[23] M. Fallanza, M. González-Miquel, E. Ruiz, A. Ortiz, D. Gorri, J. Palomar, I. Ortiz, Screening of RTILs for propane/propylene separation using COSMO-RS methodology, Chem. Eng. J. 220 (2013) 284–293, https://doi.org/10.1016/j.cej.2013.01.052.
[24] B. Schröder, L.M.N.B.F. Santos, I.M. Marrucho, J.A.P. Coutinho, Prediction of aqueous solubilities of solid carboxylic acids with COSMO-RS, Fluid Phase Equilib. 289 (2) (2010) 140–147.
[25] A. Klamt, F. Eckert, COSMO-RS: a novel and efficient method for the a priori prediction of thermophysical data of liquids, Fluid Phase Equilib. 172 (2000) 43–72, https://doi.org/10.1016/S0378-3812(00)00357-5.
[26] R.D. Chirico, M. Frenkel, V.V. Diky, K.N. Marsh, R.C. Wilhoit, ThermoML-An XML-based approach for storage and exchange of experimental and critically evaluated thermophysical and thermochemical property data. 2. Uncertainties, J. Chem. Eng. Data. 48 (2003) 1344–1359, https://doi.org/10.1021/je034088i.
[27] J.N. Miller, J.C. Miller, Statistics and Chemometrics for Analytical Chemistry, Prentice Hall, Gosport, UK, 2010.
[28] A.I. Pratiwi, M. Matsumoto, Separation of Organic Acids Through Liquid Membranes Containing Ionic Liquids, in: Ion. Liq. Sep. Technol., Elsevier, 2014: pp. 189–206. https://doi.org/10.1016/B978-0-444-63257-9.00005-5.
[29] Z. Li, Y. Cui, Y. Shen, C. Li, Extraction process of amino acids with deep eutectic solvents-based supported liquid membranes, Ind. Eng. Chem. Res. 57 (2018) 4407–4419, https://doi.org/10.1021/acs.iecr.7b05221.
[30] A.T.N. Fajar, T. Hanada, M.L. Firmansyah, F. Kubota, M. Goto, Selective separation of platinum group metals via sequential transport through polymer inclusion membranes containing an ionic liquid carrier, ACS Sustain. Chem. Eng. 8 (2020) 11283–11291, https://doi.org/10.1021/acssuschemeng.0c03205.
[31] D. Seader, E.J. Henley, Separation process principles, 2nd ed., Wiley, Hoboken, N. J., 2005.
[32] A. Maximini, H. Chmiel, H. Holdik, N.W. Maier, Development of a supported liquid membrane process for separating enantiomers of N-protected amino acid derivatives, J. Memb. Sci. 276 (2006) 221–231, https://doi.org/10.1016/j.memsci.2005.09.050.
[33] L. He, L. Li, W. Sun, W. Zhang, Z. Zhou, Z. Ren, Extraction and recovery of penicillin G from solution by cascade process of hollow fiber renewal liquid membrane, Biochem. Eng. J. 110 (2016) 8–16, https://doi.org/10.1016/j.bej.2016.02.002.
[34] S.H. Lin, C.L. Pan, H.G. Leu, Liquid membrane extraction of 2-chlorophenol from aqueous solution, J. Hazard. Mater. 65 (1999) 289–304, https://doi.org/10.1016/S0304-3894(98)00273-8.
[35] S. Leaper, A. Abdel-Karim, T.A. Gad-Allah, P. Gorgojo, Air-gap membrane distillation as a one-step process for textile wastewater treatment, Chem. Eng. J. 360 (2019) 1330–1340, https://doi.org/10.1016/j.cej.2018.10.209.
[36] C. Skuse, A. Gallego-Schmid, A. Azapagic, P. Gorgojo, Can emerging membrane-based desalination technologies replace reverse osmosis? Desalination. 500 (2021), 114844 https://doi.org/10.1016/j.desal.2020.114844.
[37] H. Renon, J.M. Prausnitz, Local Compositions in Thermodynamic Excess Functions for Liquid Mixtures, AICHE J. 14 (1) (1968) 135–144.
[38] J. Wang, J. Luo, S. Feng, H. Li, Y. Wan, X. Zhang, Recent development of ionic liquid membranes, Green, Energy Environ. 1 (2016) 43–61, https://doi.org/10.1016/j.gee.2016.05.002.
[39] E. Curcio, E. Drioli, Membrane distillation and related operations—A Review, Sep. Purif. Rev. 34 (2005) 35–86, https://doi.org/10.1081/SPM-200054951.
[40] B. Linnhoff, D.W. Townsend, D. Boland, G.F. Hewitt, B.E.A. Thomas, A.R. Guy, R. H. Marsland, Process integration for the efficient use of energy, The Institution of Chemical Engineers (1986).